PERGAMON

Solid State Communications 111 (1999) 619–624

solid state communications

Thermally reversing window and stiffness transitions in chalcogenide glasses

D. Selvanathan[a], W.J. Bresser[a], P. Boolchand[a,*], B. Goodman[b]

[a]*Department of ECECS, University of Cincinnati, Cincinnati, OH 45221-0030, USA*
[b]*Department of Physics, University of Cincinnati, Cincinnati, OH 45221-0011, USA*

Received 13 May 1999; accepted 17 May 1999 by M. Cardona

Abstract

Raman scattering and temperature-modulated differential scanning calorimetry measurements on Si_xSe_{1-x} glasses show that onset of rigidity occurs over a wide compositional window $0.20 < x < 0.27$ across which glass transitions are found to be thermally reversing in character. There is a ten-fold reduction in the non-reversing heat flow at the transition within the window in relation to that outside the window. The large compositional width associated with the onset of rigidity in this chalcogenide glass is in sharp contrast to the solitary transition predicted by mean-field constraint counting and by existing numerical simulations in random networks. © 1999 Elsevier Science Ltd. All rights reserved.

Keywords: A. Disordered systems; A. Semiconductors; D. Heat capacity; D. Phase transitions; D. Phonons

Network connectivity plays a central role in determining the physical behavior of solids. In *crystalline solids*, the effect is strikingly illustrated if one compares the physical properties of group IV (Si,Ge) with those of group VI (S,Se) elements. Even though the strength [1] of a single S–S bond (51.9 kcal/mol) exceeds that of a single Si–Si bond (42.2 kcal/mol) by nearly 20%, the higher connectivity (or coordination number, r) of crystalline (c)-Si ($r = 4$), tetrahedral network in relation to that of rhombic-S ($r = 2$), monomeric S_8 ring structure completely dominates the mechanical, elastic and thermal properties as reflected in the hardness, Young's modulus, and melting points of the two elemental solids. In covalent solids, these ideas on network connectivity were formalized using mean-field constraint counting algorithms [2,3]. These have served to distinguish [4] rigid from floppy networks *quantitatively* in terms of the excess or deficit of the average number of Lagrangian constraints per atom, $\bar{n}_c$ with respect to n_d, the number of degrees of freedom per atom ($n_d = 3$ here). Constraints come from bond-bending and bond-stretching forces, and $\bar{n}_c$ is found to scale with $\bar{r}$ as follows:

$$\bar{n}_c = 5\bar{r}/2 - 3 \tag{1}$$

Thus, a tetrahedral network of c-Si or c-Ge is intrinsically rigid because it is highly overconstrained since $\bar{n}_c = 7$ for $r = 4$, while a network of isolated rings or chains of c-S or c-Se is intrinsically floppy because it is underconstrained $\bar{n}_c = 2$ for $r = 2$. The *onset of rigidity* in a mean-field picture occurs when $\bar{n}_c$ *equals three* which according to Eq. (1) takes place from $\bar{r}_c = 2.40$.

These ideas on network connectivity have far more

* Corresponding author. Tel.: + 1-513-5564758; fax: 1-513-5567326.

E-mail address: pboolcha@ececs.uc.edu (P. Boolchand)

PII: S0038-1098(99)00248-3

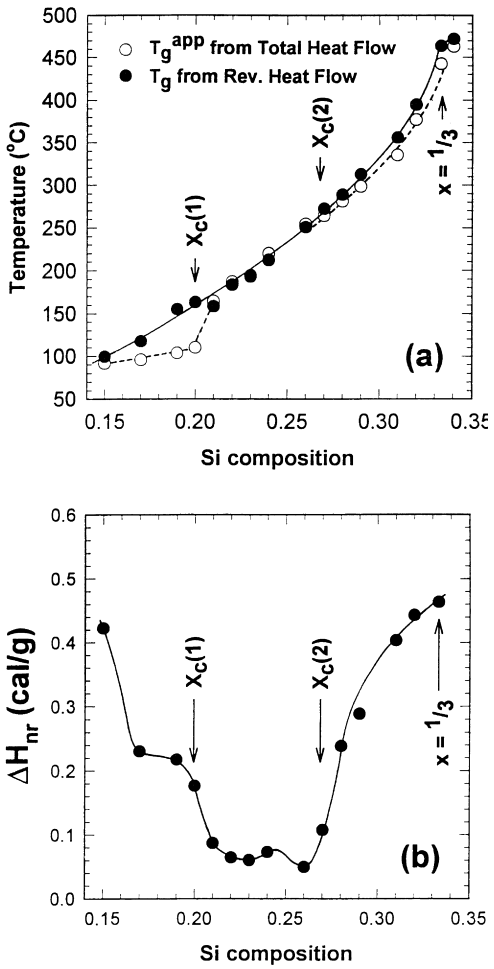

Fig. 1. (a) Shows $T_g(x)$ and $T_g^{app}(x)$ variation and (b) the non-reversing heat flow $\Delta H_{nr}(x)$ variation as a function of Si concentration x in Si_xSe_{1-x} glasses obtained using MDSC. Scan rate 3°C/min. Modulation rate 1°C/100 s. The continuous lines through the data are a guide to the eye.

profound consequences in *glasses* than in *crystals*. For example, in binary Si_xSe_{1-x} glasses, the strong valence force fields of Si and Se require these atoms to be, respectively, four- and two-fold coordinated as confirmed by experiments [5,6]. One can compositionally (x) tune the connectivity ($\bar{r} = 2(1 + x)$) in this binary glass system to approach the floppy to rigid (stiffness) transition near $\bar{r}_c = 2.40$ *continuously* by increasing x to 0.20, a luxury not feasible in crystals. The nature of the stiffness transition has evoked widespread interest [2,3,7,8] because it is generally believed that the *glass forming tendency* is *optimized* near this transition. Simulations of the stiffness transition in *random atomic networks* [9,10] show a solitary transition near $\bar{r}_c = 2.40$, with elastic constants (C) vanishing at $\bar{r} < 2.40$, and displaying a power-law behavior [10], $C \sim (\bar{r} - \bar{r}_c)^p$, with $p = 1.4$ at $\bar{r} > 2.40$. Long range van der Waals type of forces, when included in the simulations [4], give non-vanishing Cs at $\bar{r} < \bar{r}_c$.

In this communication we provide new Raman scattering and temperature-modulated differential scanning calorimetry (MDSC) results on Si_xSe_{1-x} glasses and show that rigidity occurs in *two steps*, an *onset* point at $\bar{r} = \bar{r}_c(1) = 2.40(2)$ and a *completion* point at $\bar{r} = \bar{r}_c(2) = 2.54(2)$ with a rather wide transition region $\Delta\bar{r} = 0.14(2)$ across which glass transitions are thermally reversing. These results are in contrast to the numerical simulations [9,10] on *random networks* that predict a solitary stiffness transition. The broad transition is due to the presence of a special type of medium-range structure in Si_xSe_{1-x} glasses in the transition region which is mechanically robust and retains its integrity even upon melting of the glass at T_g.

Bulk glasses were synthesized by reacting 99.9999% pure elements as starting materials in evacuated quartz ampules at 1100°C for 5–7 days. The melts were equilibrated at 50°C above the liquidus temperature, T_ℓ, for several hours prior to water quench. Since these glasses are hygroscopic they were transferred into hermetically sealed A1 pans in a dry N_2 gas ambient of a glove box for glass transition temperature (T_g) measurements using a model 2920 MDSC [11,12] from TA Instruments. Fig. 1(a) reveals the $T_g(x)$ variation deduced from the *reversing* heat flow (H_r) signal. The monotonic $T_g(x)$ increase serves as a check on glass compositions [13,14]. The observed $T_g(x)$ increase slowly at low x ($\lesssim 0.15$) starting from pure Se ($T_g = 44°C$) which can be quantitatively described by a recent stochastic model [15]. At higher x ($\gtrsim 0.15$), observed $T_g(x)$ increase more rapidly than predicted ones [15] suggesting appearance of medium-range structure. The apparent glass transition temperatures $T_g^{app}(x)$, deduced from the *total* heat flow (H_t) are also plotted in Fig. 1(a) and are found [13,14] to be less than $T_g(x)$ in general at $x < x_c(1)$ and at $x > x_c(2)$ because of a non-reversing heat flow (ΔH_{nr}) endotherm as a precursor to the glass

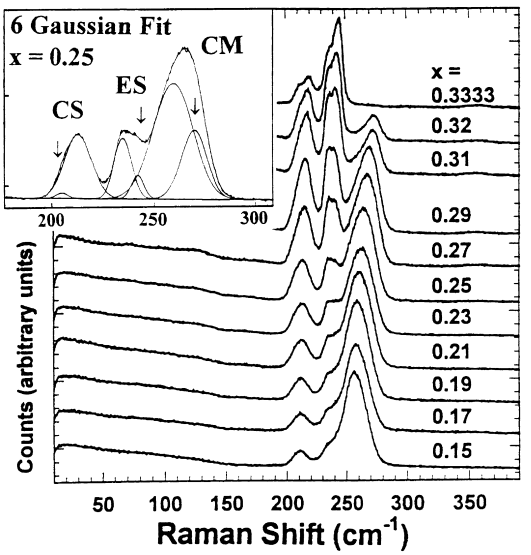

Fig. 2. Raman spectra of Si_xSe_{1-x} glasses at indicated compositions. Each spectrum is the result of nine accumulations each lasting 9 s on a CCD detector. The inset shows a least squares fit of the lineshape at $x = 0.25$ using six Gaussians to fit the three peaks CS, ES and CM indicated. Two Gaussians were used for each of these peaks, a strong (majority) mode and a weak (minority) mode. The latter are indicated by arrows.

transition. Our $T_g^{app}(x)$ trend is in good agreement with an earlier report [5,6] using DSC. The $\Delta H_{nr}(x)$ term ($= H_t - H_r$) was also measured [13,14] for the glasses and is plotted in Fig. 1(b), and reveals a deep and flat minimum in the $x_c(1) < x < x_c(2)$ concentration range. Not unexpectedly T_g^{app} approach T_g in the special composition range $x_c(1) < x < x_c(2)$ when $\Delta H_{nr} \rightarrow 0$, a point we shall discuss later.

Fig. 2 reproduces Raman spectra of the glasses at indicated compositions taken using 1.25 mW of the 647.1 nm exciting radiation from a Kr-ion laser. The back-scattered radiation was analyzed in a model T64000 triple monochromator system from Instruments, S.A. equipped with a microscope attachment, a CCD detector and recorded at 3 cm^{-1} resolution. Because Si_xSe_{1-x} glasses are hygroscopic, Raman scattering was studied in quartz tubes used to synthesize the samples. At the low laser power used, glass sample temperature deduced from the Stokes/Anti-stokes scattering was found to be about 25°C. Spectra of the glasses reveal three bands [16–18], one at 250 cm^{-1} identified as a Se_n chain mode (CM), a band at 240 cm^{-1} ascribed to edge-sharing (ES) $Si(Se_{1/2})_4$ tetrahedra, and finally a band at 210 cm^{-1} representing a symmetric stretch of corner-sharing (CS) $Si(Se_{1/2})_4$ tetrahedra. Perusal of the observed line shapes (Fig. 2) reveals that scattering strength of CS and ES units grow at the expense of CM progressively with increasing Si concentration x, and each of the underlying modes splits into doublets as x

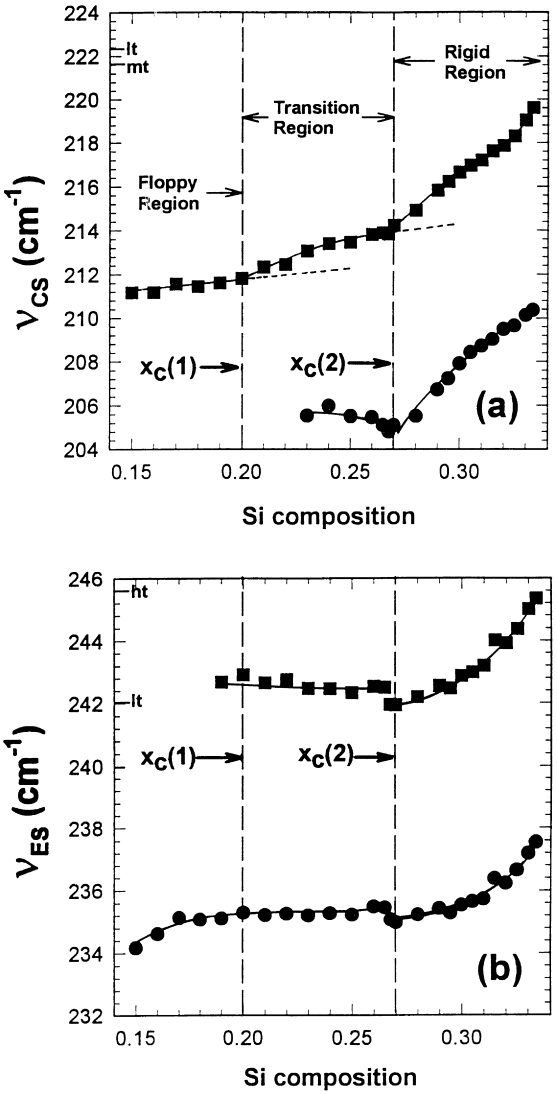

Fig. 3. Frequency variation of the (a) CS- and (b) ES-modes in Si_xSe_{1-x} glasses with Si composition. Both the majority and the minority mode frequencies of the CS and ES modes are plotted a function of x. In the least squares refinement, mode-frequency, width and scattering strength were kept unrestricted.

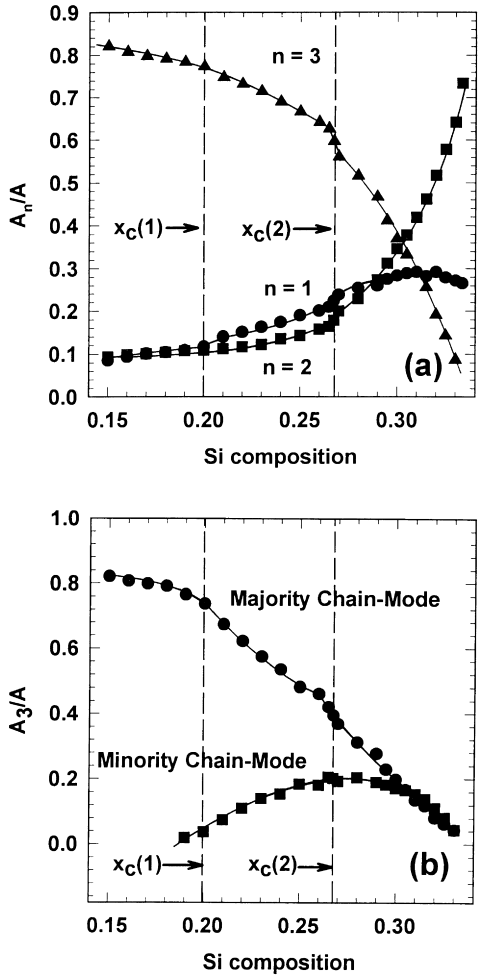

Fig. 4. (a) Raman integrated mode scattering strength ratios A_n/A for the CM ($n = 3$), ES ($n = 2$) and CS ($n = 1$) units plotted as a function of x in Si_xSe_{1-x} glasses. Panel (b) reveals deconvolution of A_3/A into the majority and minority chain-mode components.

increases to 1/3. At low x ($x < 0.19$) the observed line shapes are symmetric and can be deconvoluted in terms of three Gaussians. But at higher x ($x > 0.19$), the observed line shapes become *asymmetric* and a three-Gaussian fit becomes *inadequate*. Fig. 2 inset shows a line shape deconvolution at $x = 0.25$ in terms of six Gaussian, with each of the modes (majority) picking a companion (minority) shown by arrows. The companions are signature of medium-range structure appearing in the glasses at $x > 0.19$, and eventually lead to a narrowing and splitting of the modes as x increases to 1/3 (Fig. 2).

By deconvoluting the Raman line shapes [13,14] we have obtained the majority $\nu_{cs}^{ma}(x)$ and minority $\nu_{cs}^{mi}(x)$ CS mode-frequency variation and the results appear in Fig. 3(a). The curve of $\nu_{cs}^{ma}(x)$ shows kinks at $x = x_c(1) = 0.20$ and $x = x_c(2) = 0.27$. It is interesting to plot the CS-mode *optical elasticity*, defined as $\nu_{cs}^2(\bar{r}) - \nu_c^2$, versus $\bar{r} - \bar{r}_c$ where ν_c represents the value of ν at $x = x_c(1)$ and at $x = x_c(2)$. On a log plot we find several power-law regimes: $(\bar{r} - \bar{r}_c(1))^{p_t}$ for $x_c(1) < x < x_c(2)$, with $p_t = 0.71(10)$, $(\bar{r} - \bar{r}_c(2))^{p_r}$ for $x_c(2) < x < 0.30$ with $p_r = 1.15(10)$, and a power $p_{r'} = 1.62(10)$ in the $0.29 < x < 0.33$ composition range [13,14,19]. Parallel results for the ES mode are displayed in Fig. 3(b) and reveal both $\nu_{ES}^{ma}(x)$ and $\nu_{ES}^{mi}(x)$ to vary discontinuously near $x = x_c(2)$. The underlying optical elasticity varies super-linearly at $x > x_c(2)$ with a power $p^{mi} = 1.33(10)$ and $p^{ma} = 1.43(10)$, respectively. In Fig. 4(a), we have plotted trends in the normalized scattering strength ratio $A_n(x)/A$ for the CS ($n = 1$), the ES ($n = 2$) and the CM ($n = 3$) components. We see the suggestion of a first-order discontinuity in both A_3/A and A_2/A near $x = x_c(2)$. In Fig. 4(b), we have plotted the scattering strength variation of the majority (A_3^{ma}/A) and minority (A_3^{mi}/A) Se CM. The sum ($A_3^{ma} + A_3^{mi}$)/A appears in Fig. 4(a) as A_3/A. The majority CM is identified [13,14] with disordered Se_{3n} chains and possesses a rather broad linewidth of 22(2) cm^{-1}. The minority CM [13,14], on the other hand, has a higher mode frequency (273(2) cm^{-1}) and a narrower width (14(2) cm^{-1}) and is identified with Se-dimer or trimer linkages between CS and ES chains present in the network.

Our interpretation of these results is that rigidity nucleates at $x = x_c(1)$ or $r_c(1) = 2.40$ in CS chain-fragments (kink at $x = 0.20$ in Fig. 3(a)) which are connected by floppy Se chain segments and for that reason rigidity does not percolate at that point. At $x \geq x_c(2)$ or $\bar{r}_c(2) \geq 2.54$, the glass network undergoes a first-order transition to a percolatively rigid state and one encounters a super-linear variation of optical elasticity associated with both CS and ES modes. There is a remarkable agreement between the elasticity power-law measured ($p^{mi} = 1.33(10)$, $p^{ma} = 1.43(10)$) and the numerically predicted [9] one ($p = 1.4$) which suggests that chains of ES tetrahedra are formed at $r > r_c(2)$ and form part of the rigid backbone. The transition at $r = r_c(2)$ is first-order as suggested by

distinct breaks in $\nu_{ES}^{ma}(x)$ and $\nu_{ES}^{mi}(x)$ Fig. 3(b) as well as those in $A_2(x)/A$ and $A_3(x)/A$ (Fig. 4(a)). As x increases to $x_c(2)$, the Se–Se–Se hinge joints connecting the rigid regions are coherently depleted by Si cross-linking, driving the backbone percolatively rigid. The dual power-law $(p_r, p_{r'})$ describing elasticity of Cs modes in the rigid region probably derives from the dual chemical role of the CS units that cross-link both Se-chains and also ES-chains. It is possible that the first transition is *hydrostatic* while the second one *shear* in nature as suggested elsewhere [20]. The sub-linear power-law, $p_t = 0.71(10)$ in the transition region is reminiscent of a finite-size scaling result [21,22] which is $2/d = 2/3$ for $d = 3$ and is suggestive of long-range percolation effects.

Perhaps the most remarkable result is the existence of a wide transition region $x_c(1) < x < x_c(2)$ in the present glasses which is characterized by a vanishing ΔH_{nr}. This result follows from the optimally constrained ($\bar{n}_c \simeq 3$) nature of bonding which leads to a minimum in network stress globally and promotes glass formation. Glasses in the transition region are also the most compactly packed networks as revealed [5,6] by a broad minimum in molar volumes. The vanishing ΔH_{nr} unequivocally suggests that vitrification (cooling) or glass softening (heating) represent *thermally reversing* processes and that the *configurational entropy change* upon vitrification is actually a minimum, reflecting that the configurations sampled in the glass and liquid phases are similar [23]. This is clearly not the case at $x < x_c(1)$ where floppy Se_n-chain configurations dominate, nor at $x > x_c(2)$ where rigid ES-chains cross-linked by CS-chains have taken over.

Since $r_c(2)$ is significantly upshifted in relation to the mean-field value of 2.40, it is reasonable to suggest that the constraint associated with the weakest force in the network, the Se_n chain bond-bending force, is intrinsically broken. The fraction of Se atoms present in Se_{3n}-chains nearly halves (from 0.75 to 0.36) across the transition region, as can be seen from Fig. 4(b). Presence of a finite fraction (n_2/N) of 2-fold coordinated atoms with broken β-constraint will upshift [24,25] the stiffness threshold in a mean-field sense to a value of $\bar{r}_c$ given by Eq. (2).

$$\bar{r}_c = 2.40 + 0.4(n_2/N) \quad (2)$$

If one takes $n_2/N = 0.36$ at $x = x_c(2)$ from the plot of Fig. 4(b), one obtains $\bar{r}_c(2) = 2.54$ from Eq. (2). This remarkable agreement between the predicted (based on scattering strengths and Eq. (2)) and the observed value of $r_c(2)$ (from mode-frequency variation) provides for self-consistency of our analysis. The idea is reminescent [24,25] of the broken O bond-angle constraint in SiO_2 that upshifts the stiffness transition to $\bar{r}_c = 2.67$. An upshift of the rigidity transition from its mean-field value of 2.40 to $\bar{r}_c = 2.46(1)$ was noted earlier [19] in Raman scattering measurements on binary Ge_xSe_{1-x} glasses, although the nature of the rigidity transition appeared to be solitary.

In conclusion, Raman scattering and MDSC results on Si–Se glasses show that the onset of rigidity occurs over a wide compositional window in contrast with the behavior of Ge–Se glasses [26]. It appears that the *floppy* and *rigid* regions are separated by an *intermediate phase*, in which elements of glass structure change relatively little upon thermal cycling across T_g, as shown by the ten-fold reduction in the non-reversing heat flow (ΔH_{nr}). The network connectivity in the intermediate phase must be special. J.C. Phillips has pointed out to us the general similarity of the intermediate phase here to the intermediate phase thought to exist in the impurity band metal–insulator transition in tetrahedral semiconductors [27]. In network glasses, there are indications that the width of the intermediate phase changes with the cation and anion types in IV–VI and V–VI binary systems. An examination of the intermediate phase in such glasses may provide important clues on the role of chemical bonding configurations on the local- and medium-range structures responsible for such unusual thermal behavior.

Acknowledgements

It is a pleasure to acknowledge discussions with J.C. Phillips. This work was supported by NSF grants DMR-97-02189 and DMR-94-24556.

References

[1] L. Pauling, The Nature of the Chemical Bond, Cornell University Press, Ithaca, NY, 1960 p. 85.
[2] J.C. Phillips, J. Non Cryst. Solids 34 (1979) 153.
[3] J.C. Phillips, J. Non Cryst. Solids 43 (1981) 37.

[4] M.F. Thorpe, J. Non Cryst. Solids 57 (1983) 355.
[5] R.W. Johnson, D.L. Price, S. Susman, M. Arai, T.I. Morrison, G.K. Shenoy, J. Non Cryst. Solids 83 (1986) 251.
[6] R.W. Johnson, S. Susman, J. McMillan, K.J. Volin, Mater. Res. Bull. 21 (1986) 41.
[7] P. Boolchand, M.F. Thorpe, Phys. Rev. B 50 (1994) 10 366.
[8] M. Mitkova, P. Boolchand, J. Non Cryst. Solids 240 (1998) 1.
[9] D.S. Franzblau, J. Tersoff, Phys. Rev. Lett. 68 (1992) 2172.
[10] D.J. Jacobs, M.F. Thorpe, Phys. Rev. Lett. 75 (1995) 4051.
[11] B. Wunderlich, Y. Jin, A. Boller, Thermochim. Acta 238 (1994) 227.
[12] T. Wagner, S.O. Kasap, K. Maeda, J. Mater. Res. 12 (1997) 1892.
[13] D. Selvanathan, M.S. Thesis, unpublished, University of Cincinnati, 1998.
[14] D. Selvanathan, W.J. Bresser, P. Boolchand, unpublished.
[15] R. Kerner, M. Micoulaut, J. Non Cryst. Solids 210 (1997) 298 and M. Micoulaut (private commun.).
[16] M. Tenhover, M.A. Hazle, R.K. Grasselli, Phys. Rev. Lett. 51 (1983) 404.
[17] J.E. Griffiths, M. Malyj, G.P. Espinosa, J.P. Remeika, Phys. Rev. B 30 (1984) 6978.
[18] S. Sugai, Phys. Rev. B 35 (1987) 1345.
[19] Xingwei Feng, W.J. Bresser, P. Boolchand, Phys. Rev. Lett. 78 (1997) 4422.
[20] J.C. Phillips, in: M.F. Thorpe, P.M. Duxbury (Eds.), Rigidity Theory and Applications, Plenum Press, New York, 1999, in press.
[21] J.C. Phillips, B.D. Josephson, Phys. Lett. 21 (1966) 608 and J.C. Phillips (private commun.).
[22] J.T. Chayes, L. Chayes, D.S. Fisher, T. Spencer, Phys. Rev. Lett. 57 (1986) 2999.
[23] A. Angell, Science 267 (1995) 1924.
[24] M. Zhang, P. Boolchand, Science 266 (1994) 1355.
[25] J.C. Phillips, Solid State Commun. 47 (1983) 203.
[26] P. Boolchand, Xingwei Feng, D. Selvanathan, W.J. Bresser, in: M.F. Thorpe, P.M. Duxbury (Eds.), Rigidity Theory and Applications, Plenum Press, New York, 1999, in press.
[27] J.C. Phillips, Solid State Commun. 109 (1999) 301.